

Purdue University Purdue e-Pubs

International Refrigeration and Air Conditioning
Conference

School of Mechanical Engineering

2018

Combined Power, Cooling And Desalination Using Natural Refrigerant Powered By Low-Grade Heat Source

Praveen Kumar Govindasamy

Department of Mechanical Engineering, Anna University, Chennai, 600025, India, pravin2energy@gmail.com

Saravanan R

College of Engineering, Guindy, Chennai, India., rsaravanan@annauniv.edu

Alberto Coronas

CREVER. Mechanical Eng. Dep. Universitat Rovira i Virgili, Tarragona, 43007, Spain, alberto.coronas@urv.cat

Patrick E. Phelan

School for Engineering of Matter, Transport & Energy, Arizona State University, Tempe, AZ 85287-6106, USA, phelan@asu.edu

Follow this and additional works at: <https://docs.lib.purdue.edu/iracc>

Govindasamy, Praveen Kumar; R, Saravanan; Coronas, Alberto; and Phelan, Patrick E., "Combined Power, Cooling And Desalination Using Natural Refrigerant Powered By Low-Grade Heat Source" (2018). *International Refrigeration and Air Conditioning Conference*. Paper 2009.

<https://docs.lib.purdue.edu/iracc/2009>

This document has been made available through Purdue e-Pubs, a service of the Purdue University Libraries. Please contact epubs@purdue.edu for additional information.

Complete proceedings may be acquired in print and on CD-ROM directly from the Ray W. Herrick Laboratories at <https://engineering.purdue.edu/Herrick/Events/orderlit.html>

Combined Power, Cooling and Desalination Using Natural Refrigerant Powered by Low-Grade Heat Source

Praveen Kumar GOVINDASAMY^{1*}, Saravanan RAJAGOPAL^{1#}, Alberto CORONAS²,
Patrick E PHELAN³

¹Anna University, Department of Mechanical Engineering,
Chennai-600025, India
(E-mail: #rsaravanan@annauniv.edu)

²Universitat Rovira I Virgili, CREVER, Mechanical Eng. Department,
Tarragona-43007, Spain
(E-mail: alberto.coronas@urv.cat)

³Arizona State University, School for Engineering of Matter, Transport & Energy,
Tempe, AZ 85287-6106, USA
(E-mail: phelan@asu.edu)

* Corresponding Author: pravin2energy@gmail.com

ABSTRACT

This paper presents and discusses the combined power, cooling and desalination (CPCD) outputs operated through sustainable heat sources. The cycle, configured by heat rejection from ammonia absorption-based combined power and cycle system, is utilized for Multi Effect Distillation (MED) with Multi Stage Flash (MSF) desalination sub cycle. The triple output system operates in three different modes; power only to cooling only and cooling with power output and always with desalination output. The influence of heat source temperature, evaporator temperature and split ratio on the cycle useful outputs along with performance indicators was investigated. The proposed cycle configurations can operate by heat source temperatures as low as 125°C at -10°C evaporator temperature. Both effective first law and exergy efficiencies increase with the split ratio of refrigerant vapour mass flow rate, and reach maxima of 68.3% and 21.0% at the cooling alone condition. These grid-independent cycles are therefore suitable to provide energy intensive triple outputs using sustainable energy sources such as solar thermal, waste heat or biomass.

1. INTRODUCTION

In the past decades the scarcity and rapid rising cost of fossil fuels along with associated environmental issues have added a strong incentive for combined energy intensive production. Desalination and cooling are energy-intensive processes, and because of urbanization, climate change and increase in standard of living there are increased demand of these products. The conventional desalination methods are membrane or thermal processes. In general most desalination processes are energised by fossil fuels directly or indirectly. Similarly cooling processes are dominated by electrically driven vapor compression system. The alternate solution is generation of cooling and power through sustainable energy source technologies. Abundantly available low temperature heat sources (up to 150°C) can be converted into these energy products through thermally activated cooling technologies. Absorption is but one thermally activated cooling technology, which allows an option for both cooling and power generation by using a natural refrigerant of ammonia-water binary mixture. The special feature of this binary mixture is at subcritical pressures, with variable temperature evaporation and condensation. Since these processes, do not take place in a pure fluid, hence a binary mixture can lower pinch point with available heat source is also an added advantage (Ziegler, 2007).

To achieve higher energy efficiency, multipurpose systems can be applied in place of separate, stand-alone systems. The combined power and cooling system by using an ammonia water working pair is attractive because it can

produce both cold and power outputs from a heat source temperature of $\sim 85^{\circ}\text{C}$ (Demirkaya *et al.*, 2018). The Goswami cycle, Kalina or organic Rankine cycle integrated with absorption refrigeration cycles are foremost in absorption based power and cooling cycles. In the Goswami cycle, the simultaneous power and cooling outputs are produced in the same loop. The Kalina cycle uses an ammonia water mixture for power generation, with single-fluid power generation through the Rankine cycle. The dual output system has the ability to supply the outputs based on demand, where the power requirement is almost constant but the cooling requirement changes with time. The Goswami cycle is a power-output-based cooling system, as the cooling output is low because of sensible heat exchange with the refrigerant. The Kalina-based absorption cycle generally consists of parallel loops for power and cooling outputs. The latent heat cooling and unrectified vapor-to-power sub cycles are advantages over the Goswami cycle. In the past decades, ammonia-water-based combined power and cooling systems were thermodynamically analysed and experimentally proven by various researchers, as discussed below.

In the absorption refrigeration system, the heat rejecting components such as the condenser, absorber and rectifier, reject a substantial amount of heat to the atmosphere. The ratio of heat rejection from an absorption system compared to a vapor compression system is on the order of 2.2 (Eicker *et al.*, 2012). The performance of an absorption system strongly depends on the heat rejection system maintaining at the lowest possible temperature. Thus, wet cooling is usually preferred to operate an absorption system at higher COP. The possibility of operating an absorption system integrated with a thermal desalination system was previously studied (Kumar *et al.*, 2018). The temperature level and heat rejection capacity from an absorption system is a possible source to drive a thermal desalination system (Alarcón-padilla and García-rodríguez, 2007). Low grade heat source-operated multistage flash desalination and multi effect desalination systems are in operation worldwide.

The combined desalination and solar assisted air conditioning system was previously analysed, with the heat rejected from the condenser used for thermal desalination by maintaining at 55°C temperature (Gude and Nirmalakhandan, 2008). Under the base conditions, the heat energy available from $3.25 \text{ kW}_{\text{th}}$ cooling capacity absorption refrigeration system (ARS) is $3.45 \text{ kW}_{\text{th}}$, which produced 4.5 kg/h of fresh water through the integrated thermal desalination system. It was also claimed that the energy required for the proposed system is less than that of a multi-stage flash (MSF) distillation process. Sahoo *et al.*, 2017 proposed a polygeneration system for combined power, cooling, and desalination outputs. The cascade effect configuration system with topping cycle was intended for power generation through the Rankine cycle. The next bottoming cycle was a LiBr-H₂O absorption system, also for a power cycle. The heat rejected from the absorption cycle was utilized for a multi-effect humidification-dehumidification system. The total heat input of $21,688 \text{ kW}_{\text{th}}$ to the system produced the power, cooling and heat available for desalination of $3000 \text{ kW}_{\text{th}}$, $4700 \text{ kW}_{\text{th}}$ and $2800 \text{ kW}_{\text{th}}$. Zhang *et al.*, 2018 investigated single and double-stage NH₃-H₂O absorption system integrated with a multi effect distillation (MED) system through a cascading effect. The combined condenser and rectifier heat rejection utilized to operate the MED was, at a temperature of $\sim 70^{\circ}\text{C}$. The combined power and cooling system is a suitable candidate for integrating with thermal desalination, as the pressure ratio is a key parameter for power generation and it would be high when operating the condenser and absorber at a certain temperature difference. In order to produce the high demand products of cooling, power and desalinated water through renewable energy resources, an ammonia absorption combined power and cooling system integrated with MED desalination is proposed.

The objective of this paper is a thermodynamic study of the combined power cooling and desalination output by the integration of ammonia-based combined power and cooling cycle with an MED desalination system (CPCD). The useful output variation of the system for typical operating boundary conditions and design parameters along with corresponding performance indicators are thermodynamically analysed for the CPCD system.

2. SYSTEM DESCRIPTION

Figure 1 illustrates a schematic of the simultaneous production of power, cooling and purified water based on the ammonia-water absorption refrigeration system. The combined system is the integration of a single-stage ammonia absorption refrigeration, Kalina power and MED with flash desalination cycles. Following the stream numbering from Figure 1, the weak solution is pumped to system high pressure and it recovers heat from the solution cooled rectifier (SCR) and solution heat exchanger (stream 1 to 4). The preheated weak solution enters the generator and boils. The generated ammonia vapour from the generator (stream 8) is divided into two parts for power and cooling (stream 9 and 12). The remaining strong solution reaches the absorber after exchanging heat with SHX (stream 5 to 7). The solution cooled rectifier (SCR) rectifies part of the ammonia vapour for cooling, then it is condensed and

produces cooling in the evaporator (stream 14 to 18). The remaining unrectified vapour is used for power generation through the turbine; it is superheated before entering the turbine to extract more work without condensation (stream 9 to 11). The split ratio is the mass of refrigerant vapour for cooling sub cycle to the total generated mass of refrigerant vapor. The split ratio is used to vary the power and cooling outputs depending on demand variation. The vapour from both the cooling and power sub cycles finally reaches the absorber, in which the strong solution absorbs ammonia while releasing the heat of absorption. The total heat rejection from the absorber and condensation heat from the condenser are effectively utilized for desalination through the MED system through the cooling water circuit. The cooling water, acting as the heat rejection medium, flows in a serial manner from the absorber to the condenser and rejects heat to the desalination sub-circuit (stream C_1 to C_4). The pressurized hot water is the heat source fluid, which first exchanges heat with the superheater and then reaches the generator (stream H_1 to H_3). The mass flow rate is determined by reducing the mismatch of thermal capacitance rate in the generator. It is done by adjusting the outlet temperature of the heat source to yield the same temperature difference in both the hot and cold ends of the generator. An ethylene glycol water mixture is used as the secondary refrigerant in the evaporator to operate at less than 0°C temperature.

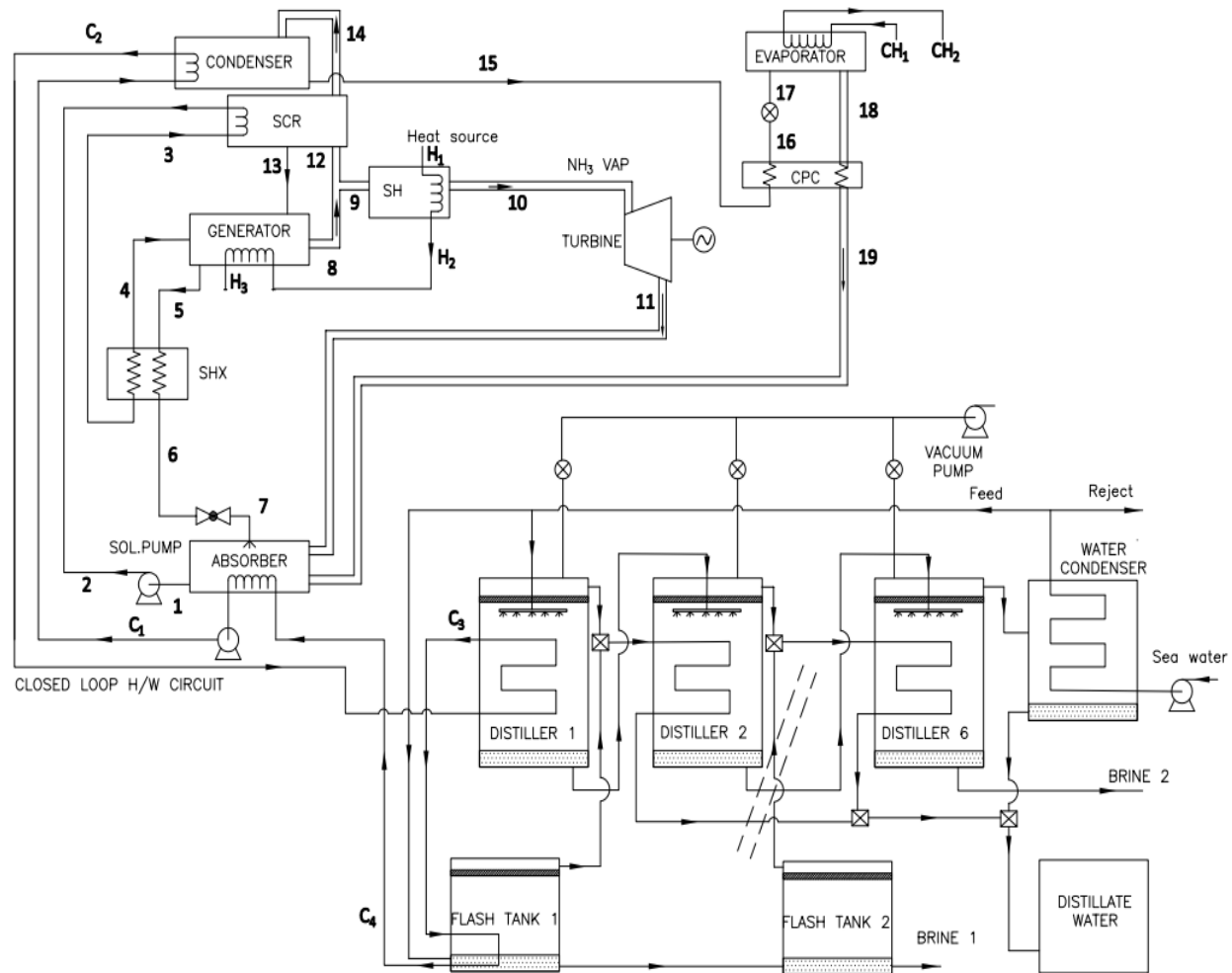


Figure 1: Schematic diagram of ammonia water absorption cycle for simultaneous power, cooling, and desalination

In the MED system, for low-temperature top-brine configuration, the forward type feed water arrangement is effective and included in the cycle configuration. The intake saline water flows into the water condenser; it exchanges latent heat with the water vapour coming from the last-order distiller and the flash system. The MED sub system consists of six distillers for vaporizing water vapour from the salt water. Over 40% of the incoming sea water rejects back and the remaining goes for flash tank 1 and distiller 1. The preheated feed water enters the first-order distiller, and is heated by rejected heat from the cooling water circuit (C_2 to C_3). The vapour generated in the first distiller rejects its latent heat to the feed-water sprayed over the tubes, and the condensed distillate is collected

through the distillate tank. Each distiller is maintained at saturated pressure for vaporization of saline water, depending on the temperature of the distiller. A portion of the preheated sea water enters the flash tank which is heated by the cooling water circuit (C_3 to C_4). The flash tank 1 is maintained at the vacuum pressure corresponding to the pressure level of distiller 1. The water vapour generated in flash tank 1 is mixed with vapour from distiller 1 before entering distiller 2. The remaining brine solution reaches flash tank 2, in which the corresponding pressure level of distiller 6 is maintained and the generated vapour enters the water condenser for condensation.

The cycle configuration can operate in three modes of operation : cooling with desalination mode, combined power, cooling with desalination mode and power with desalination mode. The variation of cooling-to-power ratio can be controlled by the split ratio (SR) of ammonia vapour to cooling and power sub cycles which directly meet the demand profiles for cooling and power. The desalination is dependent on the amount of heat generation in the condenser and absorber. In the power with desalination mode, the refrigeration sub-system is inactive, i.e, SR=0 is maintained. Likewise, for cooling with desalination mode, the power sub cycle is inactive by maintaining SR=1.

3. THERMODYNAMIC MODEL

The thermodynamic model for the system simulation and analysis is established based on the model assumptions, mass and energy balances for the individual components in the cycle. The binary mixture $\text{NH}_3\text{-H}_2\text{O}$ properties are calculated based on the correlations of (Tillner-Roth and Friend, 1998). The salt water properties are based on the correlation of Sharqawy and Zubair (2010). Both property databases are available in the external routines of EES. The physical equations for the components are also established in EES and solved for steady-state operating condition.

3.1 Model Assumptions

The following assumptions were used in the thermodynamic mathematical model (Ayoub *et al.*, 2017):

- (i) The system is operated under steady-state flow condition.
- (ii) No pressure drop in the system except at expansion valve and turbine.
- (iii) Streams of (Figure 1) 1,5,13 and 15 are saturated liquid and streams 18,9,12 and 14 are saturated vapour.
- (iv) The saturated vapour and liquid from the solution-cooled rectifier are in equilibrium at the SCR temperature and pressure.
- (v) The condenser and absorber temperature are 2°C above the cooling water inlet temperature.
- (vi) Exergy calculation is based on the reference conditions: temperature of 303 K and pressure of 1.01325 bar.
- (vii) The purified vapour from SCR is 0.999
- (viii) The isentropic efficiencies of the solution pump and turbine are 80 and 85% respectively. The effectiveness of heat exchangers are assumed as 85%.
- (ix) The distilled water from the desalination sub system is salt free.

The global mass balance for all components:

$$\sum m_{in} = \sum m_{out} \quad (1)$$

The ammonia mass balance for all components:

$$\sum m_{in} X_{in} = \sum m_{out} X_{out} \quad (2)$$

The energy balance for all components:

$$Q + \sum m_{in} h_{in} = W + \sum m_{out} h_{out} \quad (3)$$

The split ratios, SR are used to vary the mass flow rate of refrigerant vapour to the power and cooling sub-cycles.

$$SR = \frac{m_{12}}{m_g} \quad (4)$$

The specific exergy, Ex is defined as

$$Ex = Ex_{ki} + Ex_{po} + Ex_{ph} + Ex_{ch} \quad (5)$$

Kinetic and potential exergy are assumed negligible and the chemical exergy is set to zero, as no chemical loss from the cycle to the environment. Consequently, the physical exergy per unit mass of a fluid stream is expressed as

$$Ex_{ph}=(h-h_o)-T_o(s-s_o) \quad (6)$$

Table 1 provides the energy balance of the components in the CPCD system.

Table 1: Energy balance equations for each component of the CPCD system

Component	Energy balance	Component	Energy balance
Absorber	$m_1h_1 - m_{19}h_{19} - m_{11}h_{11} - m_7h_7 = m_{c1}h_{c1} - m_{c4}h_{c4}$	Solution cooled rectifier	$m_3h_3 - m_2h_2 = m_{12}h_{12} - m_{13}h_{13} - m_{14}h_{14}$
Generator	$m_4h_4 + m_{13}h_{13} - m_5h_5 - m_8h_8 = m_h h_{h2} - m_{h3}h_{h3}$	Solution heat exchanger	$m_4h_4 - m_3h_3 = m_5h_5 - m_6h_6$
Condenser	$m_{14}h_{14} - m_{15}h_{15} = m_{c2}h_{c2} - m_{c1}h_{c1}$	Condensate pre-cooler	$m_{15}h_{16} - m_{16}h_{16} = m_{19}h_{19} - m_{18}h_{18}$
Evaporator	$m_{18}h_{18} - m_{17}h_{17} = m_{ch2}h_{ch2} - m_{ch1}h_{ch1}$	Solution pump	$m_1h_1 + W_p = m_2h_2$
Splitter	$m_8h_8 = m_9h_9 + m_{12}h_{12}$	Superheater	$m_{10}h_{10} - m_9h_9 = m_{h1}h_{h1} - m_{h2}h_{h2}$
Turbine	$m_{10}h_{10} - m_{11}h_{11} = W_{exp}$	Water condenser	$m_{sw,1}h_{sw,1} - m_{sw,2}h_{sw,2} = fh_{v,i=6}$
Distiller	$m_{b,i+1}h_{b,i+1,X=0} - m_{b,i}h_{b,i,X=0} + fh_{v,i} = 0$	Flash tank	$m_{c,3}h_{c,3} - m_{c,4}h_{c,4} = fh_{v,i=6} + m_{f,1}h_{f,1} - m_{f,2}h_{f,2}$

3.2 Performance Indicators

The combined power and cooling output system performance are estimated by effective first law and effective exergy efficiency. Because cooling is low grade energy and power is high grade energy, in order to equalize both, the cooling capacity is weighted by the practical achievable COP of electrical operated cooling system, where the COP is assumed as 40% for calculation (Ayoun *et al.*, 2017).

$$\eta_{I,eff} = \frac{W_{net} + \frac{Q_{eva}}{COP_{practical}} + Ex_{Des}}{Q_{gen} + Q_{SH}} \quad (7)$$

$$\eta_{ex,eff} = \frac{W_{net} + \frac{Q_{eva}}{COP_{practical}} + Ex_{Des}}{\Delta Ex_{hs}} \quad (8)$$

The exergy for MSF desalination is calculated from the exergy difference among incoming and outgoing streams (Kahraman and Cengel, 2005).

$$Ex_{Des} = m_{dw}\psi_{dw} - m_{rej}\psi_{rej} - m_{br1}\psi_{br1} - m_{br2}\psi_{br2} \quad (9)$$

The recovery ratio is defined as the ratio between flow rates of distillate water to feed water (Farsi *et al.*, 2017).

$$RR(\%) = D_t / m_f \times 100 \quad (10)$$

Table 2: Input parameters used in the simulation

Input parameter	Value	Input parameter	Value
Mass flow rate of basic solution, m_1 (kg/s)	1	Split ratio, SR	0 to 1
Heat source inlet temperature, T_{HI} ($^{\circ}\text{C}$)	125-200	Sea water temperature ($^{\circ}\text{C}$)	25
Cooling water temperature, C_4/C_3 ($^{\circ}\text{C}$)	30/60	Sea water salinity (ppm)	35,000

4. RESULTS AND DISCUSSION

The thermodynamic performance of the combined power, cooling and desalination system is carried out up to the heat source temperature of 180°C , as this temperature level can be obtained from sustainable heat sources. The input parameters of the thermodynamic simulation are given in Table 2. Thermodynamic analysis is carried out for 1 kg/s of weak solution flow rate. The system performance is measured by the effective first law efficiency and the effective exergy efficiency for combined power and cooling outputs, while the recovery ratio is for desalinated water output. The indicators are calculated at different heat source, evaporator temperatures and split ratio. The base case performance summary of the proposed CPCD system is shown in Table 3.

Table 3: Base case performance summary of the combined power cooling and desalination system

Parameter	Value	Parameter	Value
Useful outputs		Mechanical power (kW)	
Cooling output Q_{cold} (kW_{th})	92.83	Turbine output	28.14
Net power output (kW)	24.48	Solution pump	3.66
Desalinated water (m^3/h)	3.17	Desalination subsystem	
Thermal power (kW_{th})		Heat supplied to 1 st Distiller in MED (kW_{th})	422.5
Absorber	389.7	Heat supplied to 1 st flash tank (kW_{th})	54.12
Condenser	86.92	Saline water flow (m^3/h)	1625
Superheater	6.936	Rejected sea water (m^3/h)	1424
Generator	401.3	Performance indicator (%)	
Solution cooled rectifier	27.81	Effective first law efficiency	19.39
Solution heat exchanger	324.6	Effective exergy efficiency	63.20
Condensate pre cooler	16.16	Recovery ratio	17.46

Base case condition: $T_{HI} = 150^{\circ}\text{C}$, $T_{\text{eva}} = -10^{\circ}\text{C}$, SR= 0.5

4.1 Effect of heat source temperature

The influence of heat source temperature on the cycle useful outputs such as cooling capacity, net power output and desalinated water and the corresponding effective first law, effective exergy efficiencies and recovery ratio are shown in Figure 2. The minimum driving heat source temperature for the CPCD system for the typical operating

condition is 125°C. It is found that as the heat source temperature increases, all three outputs increase. The effect of heat source temperature is more significant on net power output than on cooling and desalinated water outputs. The effective exergy efficiency is optimum at the heat source temperature of 150°C as the amount of heat supply proportion to the amount of ammonia vapour is more, (Teva=-10°C and SR=0.5) hence this optimum operating values are considered in the base case operating condition. The recovery ratio increases with increasing generator temperature as more heat is released for the same operating temperature of the cooling water circuit. The effect of flash evaporators combined with MED desalination increase the total desalination rate.

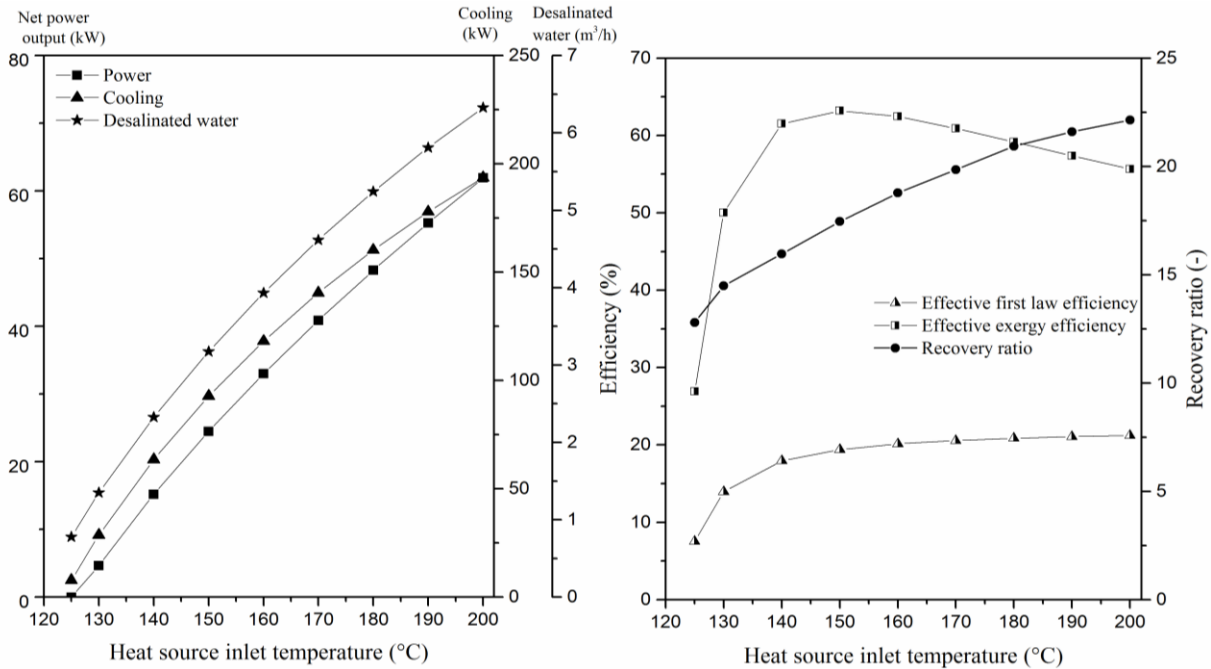


Figure 2: Effect of heat source temperature on the CPCD system (a) Cycle useful outputs and (b) Performance indicators

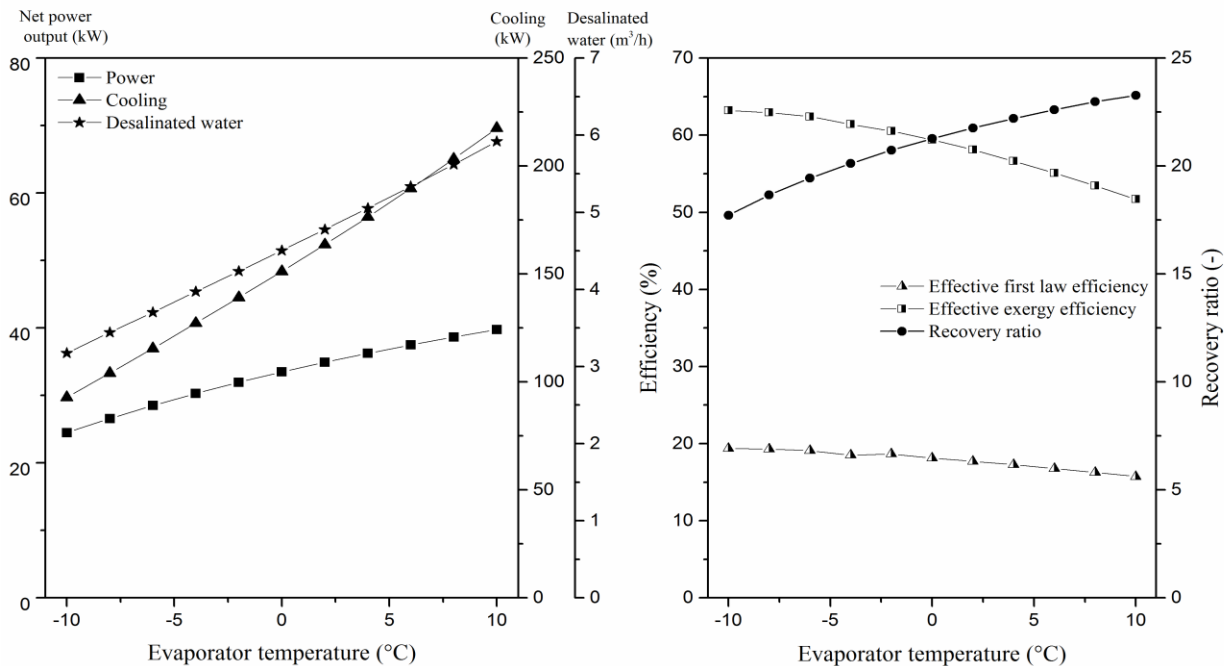


Figure 3: Effect of evaporator temperature on the CPCD system (a) Cycle useful outputs and (b) Performance indicators

4.2 Effect of evaporator temperature

The variation of cooling capacity, net power output desalination rate and the corresponding performance indicator with evaporator temperature at the base case operating condition is illustrated in Figure 3. Contrary to both the effective first law and exergy efficiencies, the recovery ratio shows an increasing trend with an increase in evaporator temperature. If the evaporator temperature rises, the ammonia concentration in the weak solution increases hence more amount of ammonia generated in the generator. This results in more cooling and power output along with high heat rejection to the desalination sub system. Even though the pressure ratio in the turbine is decreased by an increase in evaporator temperature, it is compensated and produces maximum power by more amount of binary mixture vapour flows to the turbine. It is also observed that the performance characteristics of the combined power and cooling output is decreased because of the exergy destruction in the generator increasing because of more heat and mass transfer.

4.3 Effect of Split Ratio

Figure 4 shows the variation of the CPCD system outputs and system performance for different split ratio (SR). If the split ratio is greater than 0.9, there is no net power output, as all the generated refrigerant vapor goes to the cooling subsystem. If the split ratio is between 0 to 0.9, the CPCD system runs in autonomous mode, i.e to cover the power consumption of the solution pump. As the split ratio increases, the cooling output increases as default, while it also has the effect of more heat rejection, and consequently more desalinated water production. As the split ratio varies from 0 to 1, meaning power only to cooling only with desalination output, the exergy efficiency increases steeply and it reaches a maximum at the latter condition. The effective first law efficiency also increases but not significantly. A large amount of heat rejection takes place during cooling with desalination mode, consequently more desalinated water is produced. Both effective first law and exergy efficiencies increase with the mass split ratio of refrigerant vapour, and reach maxima of 68.3% and 21.0% at the cooling-alone condition.

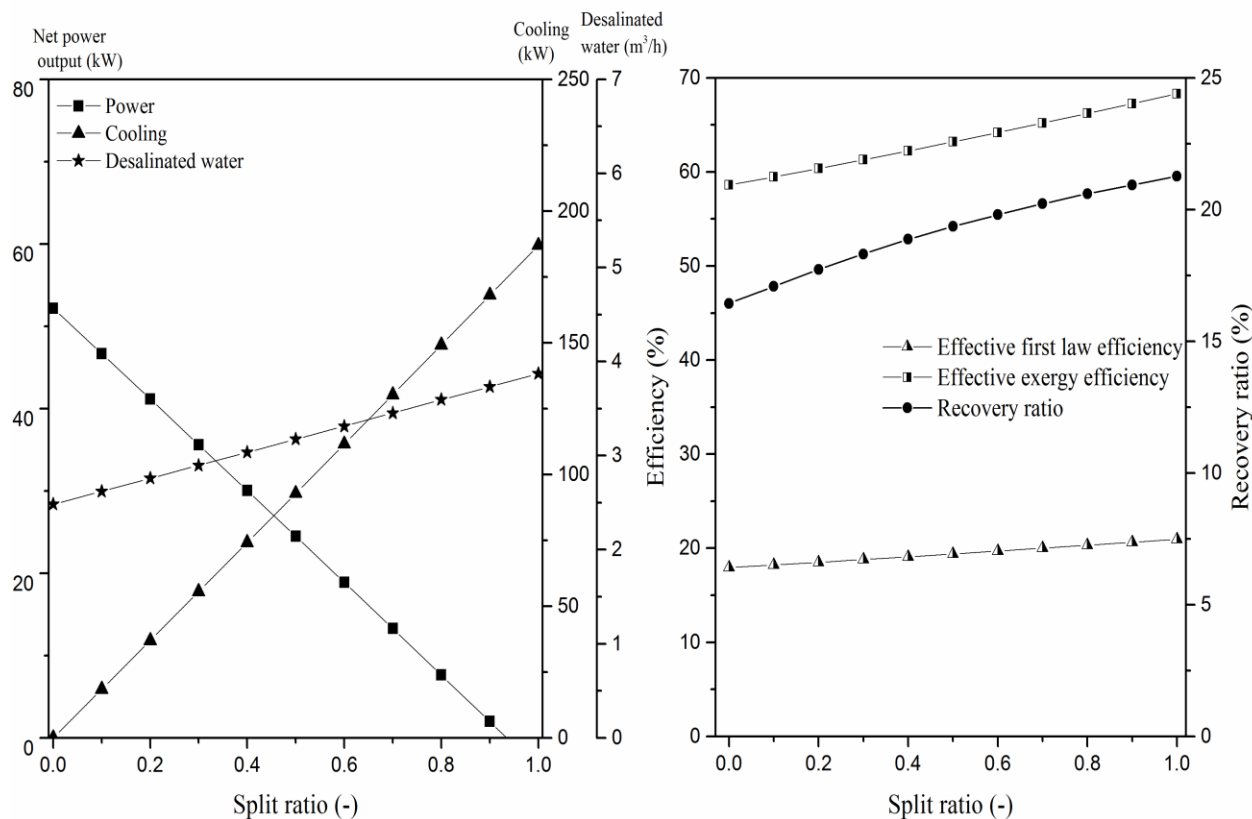


Figure 4: Effect of split ratio on the CPCD system (a) Cycle useful outputs and (b) Performance indicators

6. CONCLUSIONS

Integration of MED desalination in an ammonia-based combined power and cooling system enables high energy intensive and more demand products of cooling, power and desalinated water driven by sustainable heat sources. The thermodynamic analysis of the proposed CPCD system have been presented. If the split ratio is below 0.9, the combined output system could operate as autonomous without external electricity power. The binary mixture system is flexible to operate at various low- to medium-temperature levels. The triple output system requires a minimum driving heat source temperature of 125°C at an evaporator temperature of -10°C and it will decrease with increasing evaporator temperature. The increase in split ratio leads to increases in both effective first law and exergy efficiencies. The thermodynamic study of the proposed ammonia-based combined power and cooling system integrated with a desalination unit can also play a major role in remote areas, and it can run efficiently from sustainable thermal energy sources such as solar thermal, waste heat and biomass. Thus, the proposed CPCD system offers a sustainable approach for power, cooling and desalination.

NOMENCLATURE

m	mass flow rate	(kg/s)
h	specific enthalpy	(kJ/kg)
Q	heat load	(kW)
T	temperature	(°C)
s	specific entropy	(kJ/kg K)
W	work	(kW)
D	desalinated water	(m ³ /h)
X	ammonia concentration	
1-19	state points in the system corresponding to Fig.1	
$\eta_{I,eff}$	effective first law efficiency	(%)
$\eta_{ex,eff}$	effective exergy efficiency	(%)

Abbreviation

COP	coefficient of performance
SR	split ratio
SHX	solution heat exchanger
SCR	solution cooled rectifier
Eva	evaporator
CPC	condensate pre-cooler
RR	recovery ratio
Gen	generator
SH	superheater
C	cooling water
H	hot water
CH	chilled water
dw	desalinated water
br	brine
rej	rejected sea water

Subscript

ref	ref
in	inlet
out	outlet
ph	physical
ch	chemical
po	potential
ki	kinetic
net	net output

REFERENCES

- Alarcón-padilla, D., & García-rodríguez, L. (2007). Application of absorption heat pumps to multi-effect distillation: a case study of solar desalination. *Desalination*, 212, 294–302.
- Ayou, D. S., Bruno, J. C., & Coronas, A. (2017). Integration of a mechanical and thermal compressor booster in combined absorption power and refrigeration cycles. *Energy*, 135, 327–341.
- Demirkaya, G., Padilla, R. V., Fontalvo, A., Bula, A., & Goswami, Y. (2018). Experimental and theoretical analysis of the Goswami cycle operating at low temperature heat sources. *Journal of Energy Resources Technology*, 140(7), 072005-13.
- Eicker, U., Pietruschka, D., & Pesch, R. (2012). Heat rejection and primary energy efficiency of solar driven absorption cooling systems. *International Journal of Refrigeration*, 35(3), 729–738.
- Farsi, A., Mohammadi, S. M. H., & Ameri, M. (2017). Thermo-economic comparison of three configurations of combined supercritical CO₂ refrigeration and multi-effect desalination systems. *Applied Thermal Engineering*, 112, 855–870.
- Gude, V. G., & Nirmalakhandan, N. (2008). Combined desalination and solar-assisted air-conditioning system. *Energy Conversion and Management*, 49, 3326–3330.
- Kahraman, N., & Cengel, Y. A. (2005). Exergy analysis of a MSF distillation plant. *Energy Conversion and Management*, 46, 2625–2636.
- Praveen Kumar, G., Saravanan, R., & Coronas, A. (2018). Simulation studies on simultaneous power, cooling and purified water production using vapour absorption refrigeration system. *Applied Thermal Engineering*, 132, 296–307.
- Sahoo, U., Kumar, R., Pant, P. C., & Chaudhary, R. (2017). Development of an innovative polygeneration process in hybrid solar-biomass system for combined power, cooling and desalination. *Applied Thermal Engineering*, 120, 560–567.
- Sharqawy, M. H., Lienhard V, J. H., & Zubair, S. M. (2011). Thermophysical properties of seawater: A review of existing correlations and data. *Desalination and Water Treatment*, 29(1–3), 355–355.
- Tillner-Roth, R., & Friend, D. G. (1998). Survey and assessment of available measurements on thermodynamic properties of the mixture {water + ammonia}. *J of Physical Chemistry Reference Data*, 27(1), 45–61.
- Zhang, Z., Alelyani, S. M., Zhang, N., Zeng, C., Yuan, Y., & Phelan, P. E. (2018). Thermodynamic analysis of a novel sodium hydroxide-water solution absorption refrigeration, heating and power system for low-temperature heat sources. *Applied Energy*, 222, 1–12.
- Ziegler, F. (2007). Novel cycles for power and refrigeration. In *Proceedings 1st European Conference on Polygeneration 2007 Tarragona (Spain)* (169–182).

ACKNOWLEDGEMENT

The authors gratefully acknowledge support from the BHAVAN 2018 Internship provided by Department of Science and Technology, Govt. of India and the Indo-US Science and Technology Forum (IUSSTF) for this research.